Supporting Information

Crotti and Horowitz 10.1073/pnas.0907948106

A. wild-type *ACT1*-like

ACT1-TACTAACATCGATTGCTTCATTCTTTTTGTTGCTATATTATATGTTTAG|NNNTTGGT-*CUP1*

NNN	*PRP18*	*prp18ΔCR*
AGG (wt)	1.5	0.9
ACA	>1.5	1.2
TTG	>1.5	0.1
CAA	1.5	0.15
blank	0.03	0.01

B. 14 bases, branch point to 3' splice site (Sh)

ACT1-TACTAACATCGATTATATAG|NNNTTGGT-*CUP1*

NNN	*PRP18*	*prp18ΔCR*
AGG	1.7	1.4
ACA	1.6	1.5
TTG	1.6	0.5
CAA	1.6	0.9

C. AS1

ACT1-TACTAACATCGATTATATAG|NNNTATATTCTTTGTTTAG|NNNTTGGT-*CUP1*

NNN1	NNN2	*PRP18*	*prp18ΔCR*
TTG	TTG	0.35	0.1
"	ACA	0.75	1.2
"	AGG	0.6	0.9
"	CAA	0.5	0.8
"	GAA	0.5	1.0
"	AAA	0.8	1.4
ACA	TTG	0.07	0.04
"	ACA	0.15	0.4
"	AGG	0.1	0.25
"	CAA	0.1	0.1
"	GAA	0.1	0.25
"	AAA	0.15	0.4
AGG	TTG	0.17	0.09
"	ACA	0.5	1.0
"	AGG	0.25	0.35
CAA	TTG	0.15	0.2
"	ACA	0.5	1.2
"	AGG	0.4	0.85
"	CAA	0.4	0.9

D. AS1 variant

5' splice site AAAA|gtatgt

NNN1	NNN2	*PRP18*	*prp18ΔCR*
TTG	TTG	0.2	0.3
"	ACA	0.25	0.85

E. AS1 variant

5' splice site AAAC|gtatgt

NNN1	NNN2	*PRP18*	*prp18ΔCR*
TTG	TTG	0.45	0.1
"	ACA	0.8	0.5

F. AS1 variant

upstream splice site abolished

nn|NNN1	NNN2	*PRP18*	*prp18ΔCR*
cc|TTG	TTG	1.5	0.3
"	ACA	1.5	1.4
tt|TTG	TTG	1.4	0.1
"	ACA	1.4	1.3

G. AS2

ACT1-TACTAACATCGATTATATAG|NNNTTTTTGTTGCTATATTATATGTTTAG|NNNTTGGT-*CUP1*

NNN1	NNN2	*PRP18*	*prp18ΔCR*
TTG	TTG	0.4	0.5
"	ACA	0.4	1.1
ACA	TTG	0.1	0.1
"	ACA	0.1	0.45

Fig. S1. Copper resistances conferred by *act1-CUP1* plasmids. Single (*A* and *B*) and double (*C–J*) 3′ splice site substrates are shown. Variations in the substrates are indicated in each group. Highlighting conventions are as in Fig. 1. The results related to single site substrates (*A* and *B*) and AS1 (*C–F*) are described in the Results section. The effects of exon sequence in the AS2 substrate (shown in Fig. 1*B*, 26–29) were similar to those in AS1. In *prp18ΔCR* yeast, changing the downstream |TTG to |ACA in AS2 increased downstream splicing by three- to fivefold (comparing 26 with 27, and 28 with 29 in Fig. 1*B Left*) instead of the 10-fold increase in AS1 (Fig. 1*B Left*, 9, 10,13, and 14); in wild-type yeast, the effect of changing the downstream site was less than twofold (Fig. 1*B Right*). Changing the upstream site from |TTG to |ACA in AS2 had slightly smaller effects than this change in AS1 in both *prp18ΔCR* and wild-type yeast. Some of the results for AS2 in *prp18ΔCR* yeast suggested that other sequence elements were affecting splice site choice in AS2. The substrate |TTG–|TTG in AS2 (in *G*) conferred a higher copper resistance than *ACT1*-|TTG (in *A*), although the AS2 substrate was still sensitive to the exon bases. When the upstream site was abolished, splicing to the downstream site was normal in wild-type yeast, but was very low in *prp18ΔCR* yeast. We attributed this to unknown sequence effects. We tested restoring bases between the branch point and 3′ splice site to the wild-type ones (*I* and *J*), as compared with the bases in Sh (*B*) that were used in AS1 and AS2. The reversion to wt sequence conferred better behavior on the AS2 substrate (*I*) in that the downstream site was used properly in *prp18ΔCR* yeast when the upstream was converted to cc|TTG (comparing H and I). The AS2 variant (*I*) retained its sensitivity to both upstream and downstream exon sequences in both wild-type and *prp18ΔCR* yeast. In AS1 (*J*) in wild-type yeast, this substrate is preferentially spliced downstream, consistent with the notion that the Sh changes make the upstream site stronger. The limited sensitivity to exon sequence probably reflects the high level of splicing to the downstream site with |TTG at the upstream site. In *prp18ΔCR* yeast, exon-sequence sensitivity is maintained, and the Sh changes do not have a significant effect. The results show that the changes made in Sh strengthen the upstream site in some situations and allow us to get similar levels of splicing at the upstream and downstream sites; however, the results do not depend on the presence of the Sh mutations.

H. AS2 variant

upstream splice site abolished

nn|NNN1	NNN2	*PRP18*	*prp18ΔCR*
cc|TTG	TTG	1.5	0.03
"	ACA	1.5	0.3
tt|TTG	TTG	1.2	0.01
"	ACA	1.4	0.2

I. AS2 variant

upstream wt context restored

ACT1-TACTAACATCGATTGCTTAG|NNNTTTTTGTTGCTATATTATATGTTTAG|NNNTTGGT-*CUP1*

nn|NNN1	NNN2	*PRP18*	*prp18ΔCR*
ag|TTG	TTG	0.8	0.06
"	ACA	0.9	1.0
ag|ACA	ACA	0.3	0.55
cc|TTG	TTG	1.4	0.06
"	ACA	1.4	1.2

J. AS1 variant

upstream wt context restored

ACT1-TACTAACATCGATTGCTTAG|NNNTATATTCTTTGTTTAG|NNNTTGGT-*CUP1*

NNN1	NNN2	*PRP18*	*prp18ΔCR*
TTG	TTG	1.2	0.15
"	ACA	1.3	1.2

Fig. S1. Continued.

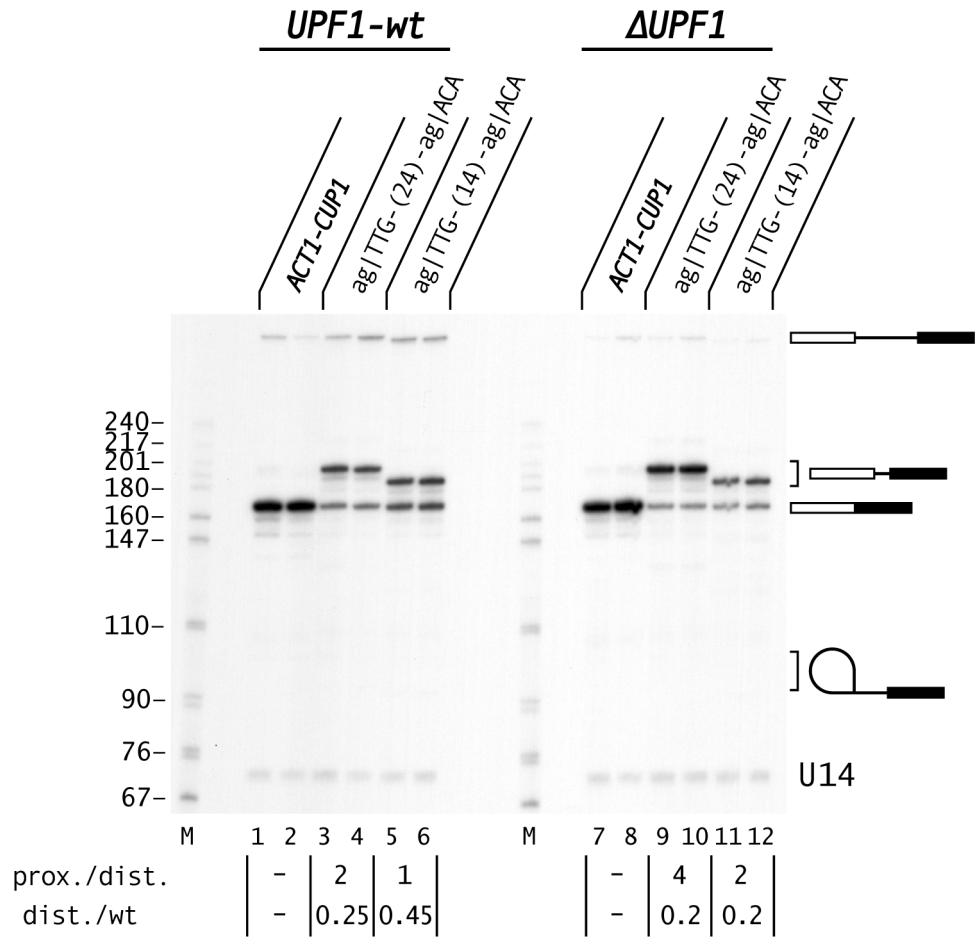

Fig. S2. Effect of *UPF1* deletion on alternative splicing. Splicing of a representative AS1-derived and AS2-derived pre-mRNA was assayed in wild-type (*Left*) and *UPF1*-knockout (*Right*) yeast. Templates for AS1 and AS2 are shown in Fig. 1*A*. The yeast had a wild-type *PRP18* allele. The spliced products were visualized by primer extension. Duplicates of each assay are shown. Splicing of wild-type *ACT1-CUP1* is shown in lanes 1, 2, 7, and 8, of AS2 ag|TTG—ag|ACA in lanes 3, 4, 9, and 10, and of AS1 ag|TTG–ag|ACA in lanes 5, 6, 11, and 12. The ratios of proximal to distal splicing and of the proximally spliced product to *ACT1-CUP1* spliced product (standardized using U14) are tabulated below the lanes; each number is the average of the two lanes. The positions of the pre-mRNA, two alternatively spliced mRNAs, lariat intermediates, and U14 standard are shown at the *Right*. The lengths of the markers (*M*) are shown at the *Left*.

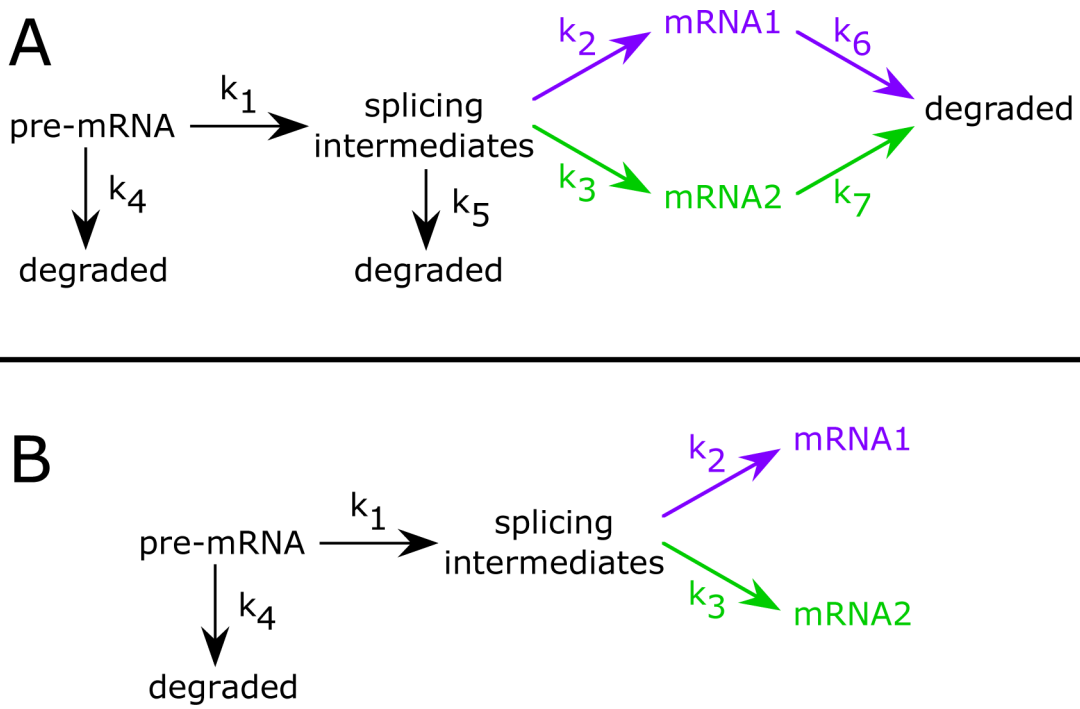

Fig. S3. Scheme for analyzing kinetics of alternative splice site selection during the second step. The scheme in *A* has a rate constant for each step of splicing and for each RNA to be degraded. Experiments show that k_5, k_6, and k_7 are small relative to the other rates and may be ignored for our estimates, leading to the scheme in *B*. In this scheme, the formation of $mRNA_1$ is given by $d[mRNA_1]/dt = k_2 \cdot [int]$. We estimated k_2 numerically using $k_2 = (\Delta[mRNA_1]/\Delta t)/[int]_{avg}$, where we compared sequential time points from quantitation of RNAs in Fig. 3 and $[int]_{avg}$ is the average [int] over the time interval (as described in figure 7 of ref. 27). Similar equations define k_3. We averaged the measured rates from the early time points of each time course to obtain our rate constant estimates. The rate constant is the ratio of the rate of formation of the mRNA to the concentration of intermediates. Thus, in Fig. 3*B*, the ag|TTG–cc|TTG transcript has a higher level of intermediates than the other transcripts, and a correspondingly higher rate of formation of mRNA (leading to more mRNA) even though the rate constant for splicing to the proximal (upstream) site is the same as in the other transcripts, which have less intermediate (because of splicing to the other sites) and hence less proximal splicing. We note that this kinetic scheme predicts that the ratio of $[mRNA_1]$ to $[mRNA_2]$ will be constant (equal to k_2/k_3) over time, and we observe this constancy in all of the time courses in Fig. 3. We assessed whether the first step was affected by comparing time courses of the total amounts of RNAs that have passed the first step (that is, the sum of the molar amounts of intermediates and mRNAs) and by checking that the decay rate for the pre-mRNA given by (k_1+k_4) is similar for the transcripts. For the transcripts shown in Fig. 3, we observed very similar apparent first step rates.

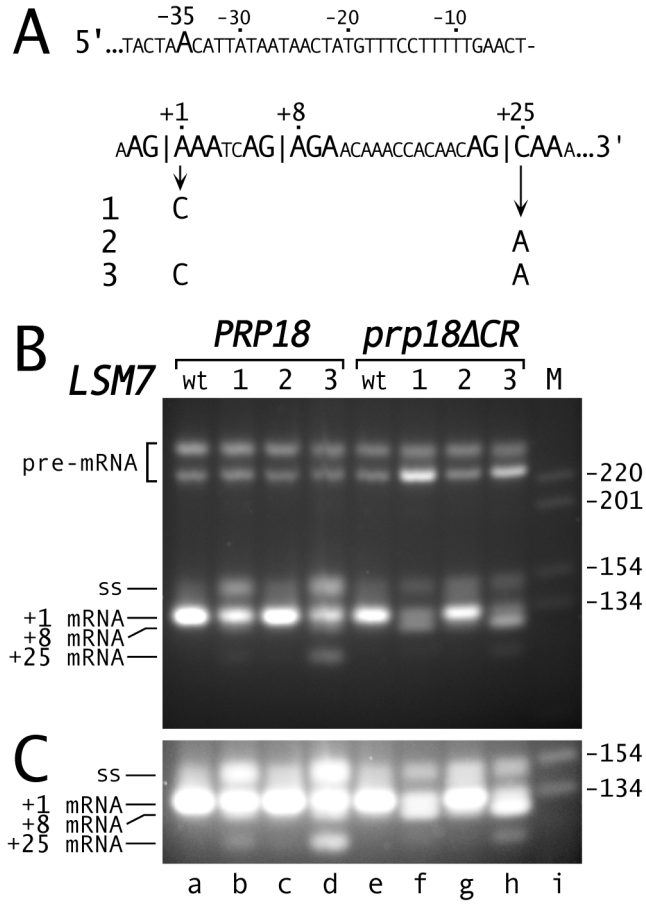

Fig. S4. RT-PCR analysis of the effect of exon mutations on the splicing of *LSM7*. (*A*) Sequence of the 3′ splice site region of *LSM7*, emphasizing the branch site at −35 and two downstream AG dinucleotides. Three *LSM7* mutants are shown. (*B* and *C*). RT-PCR analysis of splicing of wt *LSM7* and the three mutants in *PRP18* Δ*UPF1* and *prp18*Δ*CR* Δ*UPF1* yeast. Alleles of *LSM7* are indicated at the top. This figure shows an RT-PCR analysis of the same samples shown in Fig. 4 *B* and *C*. *C* is a longer exposure of the same gel as in *B*. The positions of DNAs corresponding to the pre-mRNA and mRNAs are indicated. The band labeled ''ss'' is thought to be a mixture of single-stranded DNAs. After RT, PCR was carried out for 25 cycles, and the DNAs were separated on an agarose gel. The RT-PCR analysis is not expected to be quantitatively accurate, but the +25 mRNA products in lanes b, d, and h are easily visible. Bands were identified by sequencing of gel-purified DNAs.

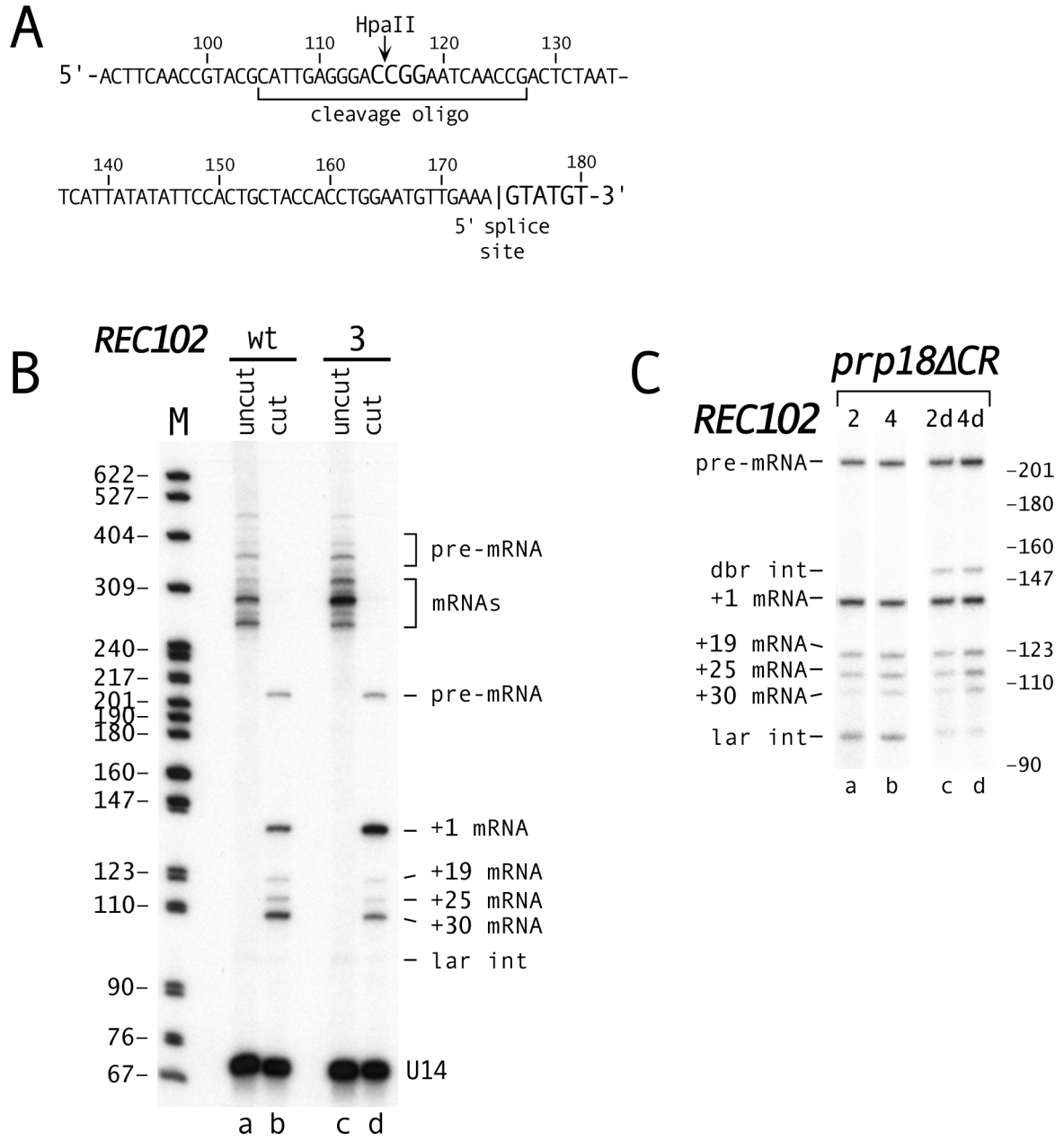

Fig. S5. Digestion of *REC102* primer extension products with HpaII and identification of *REC102* splicing intermediate. (*A*) Sequence of *REC102* upstream of the 5′ splice site. The bases are numbered from the ATG start codon. The positions of the oligo used for cleavage, of the HpaII site, and of the 5′ splice site are shown. (*B*) Primer extension reactions of *REC102* wild-type (wt) and mutant 3. RNAs were made from *PRP18-wt ΔUPF1* yeast. Lanes a and c show the primer extension reaction products, and lanes b and d show the products after annealing with oligonucleotide and cutting with HpaII. The uncut products correspond approximately to the expected sizes of 265–294 bases for spliced mRNAs (depending on the site used) and 362 bases for pre-mRNA. The faint lariat intermediate band is not cut. We are not able to account clearly for the extra bands in the uncut primer extension reactions. After cutting, no extraneous products are seen (lanes b and d). We imagine that a second, upstream promoter has been created in our construction, leading to the complexity and its complete resolution by cutting. (Such a promoter could also account for the band ''y'' in the *LSM7* primer extensions in Fig. 4*C*.) We also used a second oligonucleotide (data not shown) complementary to bases 139–165 that includes a BtsI site; cutting with BtsI produced a pattern identical to HpaII with shorter DNAs. RT-PCR of the primer extension reactions using the primer extension oligonucleotide and an oligonucleotide at the expected start site gave several products with a pattern reminiscent that seen in lanes a and c. Gel purification and sequencing of each product (with both PCR primers and an internal primer) showed only the sequences expected for the primer extension products. Labels are as in Fig. 5*B*. (*C*) Total RNA from *prp18ΔCR* yeast with REC102 mutants 2 and 4 was treated with Dbr1 before primer extension, causing a reduction in the amounts of lariat intermediate (lar int) and the appearance of a new band (dbr int) of the expected size. Primer extensions of untreated RNAs are shown in lanes a and b, and of Dbr1-treated RNAs in lanes c and d. *REC102* primer extension products are labeled as in Fig. 5*B*. *C* was assembled from one uniformly adjusted exposure.